A SunCam online continuing education course

Forensic Engineering – Part C

Case Histories: Metallurgical & Mechanical Failure Analyses

By

Gerald O. Davis, P.E.

Introduction

This course is intended to illustrate, with (6) case histories, some of the principles and approaches to completing root-cause failure analyses (RCFA) that were presented in the author's previous Suncam courses: *Forensic Engineering Part A and Part B* as well as *Corrosion Control and Tactics*. Those courses, as well as this one, were focused on metallurgical and mechanical RCFA's. The several forms of metal failure by corrosion are, of course, important aspects of the broader area of metallurgical failures. Here it is assumed that the reader is either generally familiar with the contents of these previous courses <u>or</u> has had engineering experience analyzing failures that involved metallurgical and mechanical issues.

Selected aspects from the three categories of metallurgy, corrosion and mechanical engineering are presented in the cases. Often information from more than one of these categories is needed for a given case. Problem solving generally follows the Scientific Method.

Most of the case histories are actual RCFA's but the names of the actual participants, brand names, equipment numbers and other identifying information have been omitted and replaced with generic information to protect all involved.

Some of these cases involved (or could have involved) legal actions. However, those aspects are not discussed here. Instead, the discussions focus on the technical aspects of establishing the most viable and supported physical cause for the given failure and on recommendations to prevent a recurrence.

For each case the sequence of discussion, in general accord with the Scientific Method of problem solving, is applied as follows:

Introduction and Background
Statement of the Potential Failure Mechanisms Evaluated
Investigations and/or Testing
Results of the Investigations and/or Testing
Conclusions
Recommendations to Minimize Chances of a Recurrence

Following the cases is a short list of additional examples of engineering problem situations, among <u>many</u> others, that a failure analyst might encounter. This is offered, along with the detailed cases, to show the diversity of what is called forensic engineering or root-cause failure analysis when confined to metallurgical and mechanical engineering topics.

Case 1- Superheater Tube Failures in a Large Steam Boiler

Several years ago, a chemical manufacturing plant had three, oil-fired electric power utility size steam boilers (designated here as #'s 1, 2 & 3) that were used to produce process heating steam but not electric power. The boilers were water-wall types with water-wall tubes mounted inside outer, insulated steel walls that were surrounded by a large vertical structure. Figure 1 is a simplified, schematic representation of the overall configuration, water-to-steam flow path and primary components of the single boiler involved in this case. That boiler was #1.

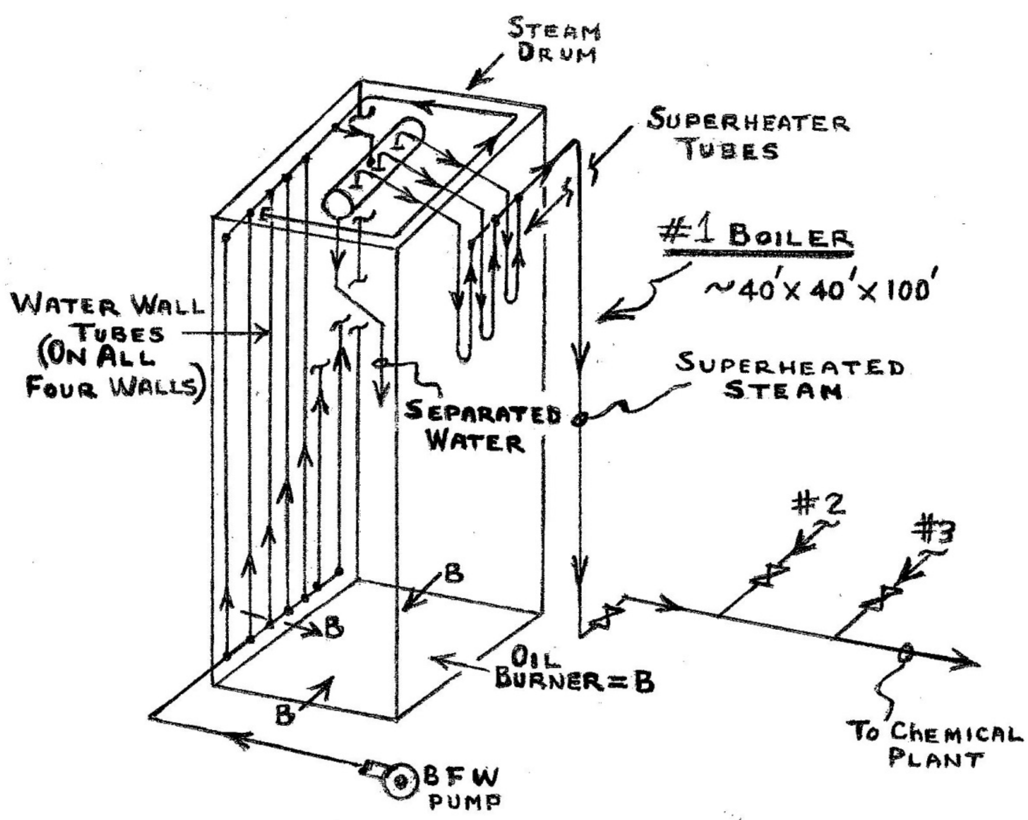

Figure 1 – Simplified Schematic Drawing of Boiler # 1 and Essential Components

For economic operation, the plant had to run on a 24/7 basis. The normal steam outputs of all three boilers were needed to meet the chemical plant's steam requirements. Boiler #1 was the oldest and had the largest output capacity of the three boilers. If any superheater tubes failed because of rupture in #1, they were plugged during a brief shutdown. That boiler was then re-started at an increased fuel oil firing rate to make the previous steam output. However, the needed additional fuel oil presented added cost.

NOTE: No boiler water wall tubes were involved in this RCFA. Therefore, from this point forward, whenever tubes are mentioned, that should be understood to mean superheater tubes.

Over a recent three month period, four tubes failed and had to be plugged . Three other tubes in #1 had been previously plugged during the first years after start-up. Also, three bulged, but not yet ruptured, tubes were found during a recent shutdown of #1. Most of the seven failed tubes plus the bulged tubes were all located in or near the north end of the boiler's fired combustion volume. The chemical plant's reliability engineering department was directed to conduct a root-cause failure investigation of Boiler #1 to define the cause of the tube problems and to make recommendations.

The analysis began by gathering current and historical information for #1 by reviewing specifications, drawings and past reliability engineering inspection reports plus personally interviewing the relevant operations and maintenance personnel. Sample sections of tubes were removed that included those that: (a) had been plugged, (b) bulged but not ruptured and (c) also some that were "good" and apparently had suffered no significant problems. Loosely held and randomly distributed, thick, solid deposits were found on the external surfaces of each of three types of tubes. Varying levels of thin, tightly held black deposits were seen at various locations inside both the failed and bulged tubes, but little or no such deposits were found inside the "good" tube samples. It had been nine years since Boiler #1 had been chemically cleaned to remove internal deposits.

The black deposits in the bulged tubes were primarily located immediately around the bulged areas. The failed tube samples had fish mouth-shaped openings parallel to the longitudinal axis of the tubes. The sizes of the openings varied from 2 X 3/8 inches to 4 X 3/4 inches.

Samples of both the external and internal deposits were sent to a lab for chemical analysis. Metal samples of all three types of tubes were sent to a metallurgical lab to identify the chemical composition of the metal. Comparative metallographic examinations of the three tube samples were also requested, to determine if their microstructures revealed reasons for the failed and bulged tubes versus the "good" tube sample. The tube material was specified to be ASME SA-192. This is a plain carbon steel with no additional alloying elements, such as molybdenum (Mo) or chromium (Cr), that increase the heat resistance of the material. Boilers commonly use SA-192 steel but usually for water-wall tubes and not for the higher temperature exposures of superheater tubes.

Consideration of the possible failure mechanisms for evaluation focused on two areas. One was overheating of the steel tubes along with oxidation and the related loss of strength. The other was the high temperature mechanism of creep leading to creep-rupture. Creep is time-dependent plastic (permanent) strain produced at a constant stress and high temperature. Creep-rupture is the eventual fracture of a material subject to creep after a particular time at a given stress. It was unknown why the failures and bulges were confined to only some tubes.

Overheating might logically be related to the deposits, external and internal, found on and in the affected tubes. The interviews and research of past inspection reports on #1 provided two possible sources of overheating and creep in selected tubes. The first possibility was what were called "flying restarts" after #1 had to be shut down due to temporary loss of electric power that supplied several motor-driven pumps needed for boiler operation. For unknown reasons, temporary electrical power interruptions were confined to Boiler #1. This was a separate problem scheduled to be evaluated as another RCFA. The normal outputs of all three boilers were needed to meet the chemical plant's steam requirements, so flying restarts of #1 were judged to be necessary until the electrical supply issue was solved.

During a "flying restart", oil burners in #1 were restarted with high oil feed rates to increase flue gas temperatures as quickly as possible in the boiler's fired cavity. Thus, temperatures increased outside the tubes with no internal steam flow because the main valve, located between the boiler's outlet and the inlet to the header pipe that fed steam to the plant from all three boilers, had to remain closed (see Figure 1). This was necessary until the pressure of superheated steam made by #1 had built up to the 425 psig level of boilers # 2 and #3. During normal operation, full steam flow at 425 psig inside the tubes acted to remove heat from those tubes' walls and keep them at a reasonable temperature. However, during typical flying restarts, tube walls were temporarily heated to much higher temperatures than they would experience under normal operation. The extent of the thermal effects of these flying restarts on the tubes was uncertain.

The second potential cause of overheating and creep of the tubes was related to the separators inside the steam drum of Boiler #1. These were closely spaced steel plates that were intended to separate most of the water from the saturated steam that entered the steam drum from the water wall tubes before exiting to the superheater tubes. Different banks of separators fed different outlets from the steam drum and thus different tubes. During a past major maintenance shutdown of #1, it had been found that some of the separator plates, primarily in the north end of the steam drum, were out of alignment so that partial blockage of outlet steam flow occurred. At the time, the extent of this effect was not judged to be significant so no corrections were made. Because of partial blockage of some separators, the cooling effect of steam flow in affected tubes could have been reduced significantly. This would have occurred continually during normal boiler operation.

Besides the laboratory tests of tube deposits and metallurgical analyses of the affected tube's steel, detailed heat transfer calculations were completed. The goal was to determine if the maximum temperatures reached by the tubes would significantly reduce their strength and susceptibility to creep-rupture. It was assumed that the external deposits provided some extent of insulation to the tubes from the boiler's high temperature combustion gases. Simultaneously, internal tube deposits acted as insulators to prevent maximum cooling of tube walls due to steam flow inside the tubes. The effects of convection and radiation from external combustion gases to the outside surface of the tubes were considered along with conductive heat transfer through the interface of external deposits, the tube wall itself and the internal tube deposits to the flowing steam. Clearly, several assumptions were needed to complete the calculations.

Results of the analysis of the external tube deposits showed that they consisted of vanadium oxide, magnesium oxide and iron oxide. Most of the latter was directly next to the tube surface. This combination was, as expected, the combustion products of burning the #6 fuel oil that had always been used in the boiler. Vanadium is normally in this fuel oil and magnesium was used as an additive to the oil to promote better combustion. There was no evidence of significant corrosion pitting of the external tube surface under these deposits. The internal, thin black deposits were magnetic and found to be essentially all iron oxide. Iron oxide could have been created when some of the residual water, along with the steam entering a given tube, encountered a hotter than normal inner tube surface, broke down into hydrogen and oxygen, allowing the free oxygen to react with the steel to form iron oxide. This reaction occurs at about 930^0 F. Over time, thin variable deposits of iron oxide would have formed. This likely occurred while most of the residual water immediately flashed to steam.

The metallurgical analyses of the steel in three types of tubes indicated overheating in both the failed and bulged tube samples. Specifically, metallographic examinations of polished and etched cross-sections of the steel included clearly enlarged grain sizes, decomposition of pearlite into ferrite plus spheroidal carbides and excessive general oxidation. These results would indicate overheating to a temperature of at least 1350^0 F. The "good" tube sample had only very minor indications of raised temperature exposure.

There were two primary problems in obtaining valid heat transfer results. One was in finding reliable conductivity values for the external and internal deposits after establishing their compositions. Very little information on these conductivity values was available. Thus, the approach used was to repeat the calculations using different conductivity values that appeared probable based on available information and then determine the range of resulting maximum tube wall temperatures. The second problem was how to address the occurrence of unsteady steam flow rate periods and their duration in the tubes. There were no clear answers for this. Instead, the assumption necessarily was the much simpler situation of full, steady state steam flow in the tubes. This would provide maximum cooling effect on the tubes being heated externally by high temperature combustion gases. It was understood that this assumption would result in a range of calculated tube temperatures (based on the values of conductivity used) that were less than the actual temperatures. Even so, it was assumed that the heat transfer calculations would provide a useful basis for comparison with other findings.

Using the required shortcomings inherent in the heat transfer calculations, the maximum predicted tube temperatures ranged from 758 to 1018^0F, but for the above reasons, this range was very likely lower than reality. How much lower was unknown. The ultimate tensile strength (UTS) of plain carbon steel decreases rapidly at temperatures above approximately 400^0F. For example, at 1350^0 F, the steel's UTS is about 5,000 psi. A temperature of 1350^0 F is the minimum value the steel had to have been exposed to while in service, according to the results of the metallographic study of the failed and bulged tube samples. Thus, it is likely that these tubes reached temperatures above 1350^0 F, and at such temperatures, their UTS would be less than 5,000 psi. The calculated applied service stress in the 2-inch diameter tubes, with an original wall thickness of 0.175-inch and normal internal pressure of 425 psig, was 2,363 psi, as per the ASME Code, Section I, in PG-27.2.1. Oxidation at higher temperatures would decrease the tubes' intact wall thicknesses below 0.175- inch and increase the applied service stress above 2,363 psi, therefore getting closer to the UTS of the steel.

Data on the creep-rupture of plain carbon steel, such as the SA-192 tube material, was obtained from ASTM Technical Publication No. 180. This showed that at an assumed service stress of 2,363 psi (from above) and a temperature of 1018^0 F (maximum value via the heat transfer calculations) would result in creep-rupture in about 11 years. However, if the stress remained the same but the temperature changed to 1350^0 F the time to creep-rupture was drastically reduced to about 6 days. This shows the major effect of increased temperature on the point of creep-rupture of plain carbon steels containing no alloying elements to resist high temperature effects.

In conclusion, the affected superheater tubes failed by a combination of high temperature exposure, oxidation and creep-rupture. It is unclear which effect was more deleterious in causing the failures and bulges. The unusual high temperatures were caused by internal iron oxide deposits in the tubes, the flying restarts and the partially blocked separators previously found in the north end of the steam drum. The internal deposits very likely had the largest role in causing the problems. The relative importance of damage due to the flying restarts and separators was unclear. The location of the deficient separators explained why the north end of the group of tubes had most of the failed and bulged tubes.

Recommendations made may be summarized as follows:

- Chemically clean the boiler to remove the iron oxide deposits in all superheater tubes and repeat this every five years, given the marginal high temperature-resistance of the many already installed SA-192 tubes.
- Replace all previously plugged tubes to re-establish the original number of tubes and boiler efficiency.
- Decrease the initial fuel oil firing rates during a restart after a power interruption to produce slower increases in tube temperatures and permit more time for steam pressure to build.
- Immediately investigate and correct the "unique" electrical problem in this boiler system that causes shutdowns due to loss of electrical power.
- Finally, correct any damaged or misaligned separators in the steam drum.

Taken together, these actions should re-establish the reliability and economic performance of Boiler #1.

Case 2 – Corrosion of Aluminum Sheet Pilings at a Boating Marina

Aluminum (Al) sheet pilings in one section of a boating marina showed abnormal and severe corrosion. This section was about one-hundred feet in length and had been in service at the location <u>for nine years</u>. The marina was on a river about one mile from the ocean, so the water there was brackish and not seawater. Initially, there was no notable corrosion, but in the last year it became clearly visible. Another section of the same type and length of Al sheet pilings had much less corrosion, but both were installed at the same time. Both sections of pilings had their lower vertical sections exposed to the same brackish water and to the same atmospheric air conditions above the water level.

The appearance and pattern of the severely corroded piling section was unusual in that each attack site was pit-like in appearance but relatively large in diameter, widely spaced from others and with considerable corrosion product in the pits. This is not like the typical pitting corrosion sites that can appear on Al alloys; those are generally small in diameter, closely spaced and show only small amounts of corrosion product. The latter conditions existed on the nearby piling section that had only minor pitting. It had been in that much less severe condition for several years and was not a concern.

The installation configurations of the two piling sections were not the same. Both were immediately adjacent to concrete pads on which cars and boat trailers were parked at the marina. However, small traffic barriers at the edges of the concrete pads and above the vertical sheet pilings were different. At the severely corroded piling section, the traffic barrier was concrete and cast along with the adjacent concrete pad. The traffic barrier, at the piling with only minor corrosion, consisted of aluminum plate that had been formed into the same shape as the concrete barrier and then bolted on to its adjacent concrete pad. Figure 2 provides a sketch of the vertical sheet piling, concrete parking pad, traffic barrier and high tide water level at the piling section with the unusual and severe corrosion. The other section with minor and typical pitting corrosion was essentially the same, except for use of an aluminum traffic barrier.

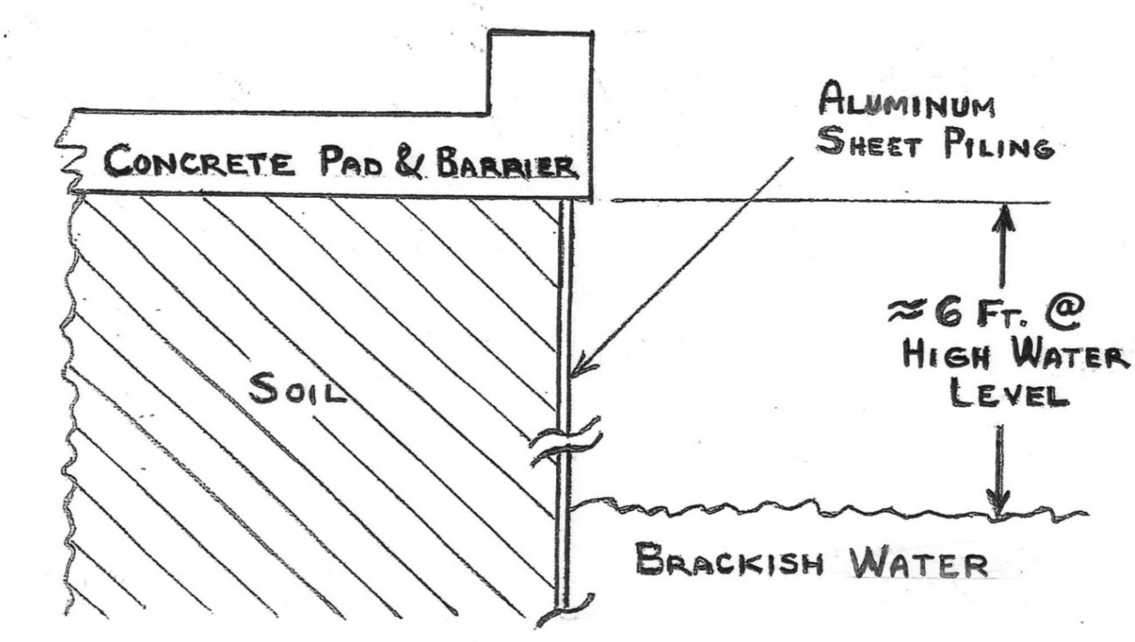

Figure 2 – Cross-sectional Sketch of Aluminum Sheet Piling Adjacent to the Concrete Pad and Traffic Barrier at the Marina

The failure analyst was requested to find the root cause of the severe corrosion on the one section of pilings and make appropriate repair recommendations to prevent its recurrence.
It was clear that a type of pitting corrosion was occurring at the piling section with the severe level of attack. The detrimental effects of chloride ions in the water and atmospheric air at the marina were assumed to be important to the condition seen. The critical question was why this pitting was so different in both characteristics and degree, versus the minor pitting seen on the other aluminum piling section. The concrete traffic barrier was judged to be a factor in the corrosion, but just how it affected the process was unclear. It was also uncertain why the severe corrosion had taken so many years to develop.

An investigation showed that the aluminum alloy specification at both piling sections was 6061-T6. This is a commonly used Al alloy that typically has relatively good corrosion resistance in many types of service. On-site inspection of the piling in question indicated general confinement of the corrosion to the sheet surface starting about three to four feet above the high-water level and extending up to just under the slight overhang of the traffic barrier. Thus, there were very few attack sites close to the high-water level, and none were visible below the water level. Inspection also showed that the pit-like attack sites were generally conical in shape with the larger diameters next to the water side of the piling and the more pointed end of each cone-shape closer to the soil side. This confirmed that the corrosion on the piling originated from the water side and not the soil side.

Review of corrosion sources indicated that aluminum alloys can be susceptible to accelerated corrosion of several types when certain chemical conditions exist either in the service environment or as consequences of alloying elements in the Al itself. The latter is well known, and so, there are limits defined for allowable levels of particular elements in each Al alloy specification. In 6061-T6, these critical alloying elements are copper, iron and lead. The contents of solid corrosion products depend on the type of corroded metal as well as the elements present in the service environment. The latter elements, in the form of ions, which can be detrimental in promoting corrosion in the service environment of this case, would be chlorides, lead and mercury. If the concrete was involved in this severe pitting then calcium, as a primary element of the lime in the concrete, would be important to identify as present in the solid corrosion product.

Aluminum alloys have a somewhat unique characteristic in that they are most resistant to corrosion when exposed to service environments with pH values near neutral, e.g., slightly above and slightly below pH = 7. But they may suffer accelerated attack at <u>both</u> very low (acidic) pH values and very high (alkaline) pH’s. For this case, the likely condition was low pH values. The pH of both the brackish water and the corrosion products found on each attack site could be important in establishing a root cause of the severe corrosion seen. The pH of corrosion products will generally depend on the pH of the service environment. However, a specific feature of pitting corrosion in a chloride-containing environment – like this brackish water – is that the pH of the corrosion product in pits becomes much more acidic than that of the service environment.

Multiple samples of the brackish water and of solid corrosion products were collected for laboratory analyses. Testing determined the pH of the water, along with the concentrations of chloride ions plus copper, calcium, lead and mercury in the water. Testing also determined the pH of the corrosion products, along with the concentrations present of chlorides, copper, calcium, iron, lead and mercury. It was found that the specification for aluminum alloy 6061-T6 defines the maximum permitted concentrations of copper, iron and lead that may be present in the metal. The objective in obtaining this information on 6061-T6 was to compare the maximum allowed values of these three elements to their concentrations found by analysis in the corrosion products. If the concentrations of these detrimental elements in the corrosion products were higher than permitted by the specification for this aluminum that would indicate this particular aluminum was defective.

The results of these lab analyses were as follows (concentration units are in parts per million, ppm):

Evaluated Parameter	**Brackish Water**	**Corrosion Product**	**Max. Allowed for Al 6061-T6**
pH	7.5	4.38	N/A
Chloride	14,800	13,200	N/A
Copper	BQL	640	4,000
Iron	N/A	1,100	7,000
Calcium	N/A	7,700	N/A
Lead	BQL	100	500
Mercury	BQL	BQL	N/A

BQL = Below Quantitative Limit of the analytical detection method used
N/A = Not Applicable for analysis

These data confirmed several facts relevant to the failure. Most important was the high levels of both chlorides and calcium in the corrosion products. A search of relevant corrosion references indicated that calcium chloride ($CaCl_2$) is very aggressive in promoting corrosion of aluminum alloys. This compound would naturally form given the large amounts of both of its chemical components being present in the corrosion product. Other findings were also significant. The fact that the pH of the corrosion product was so much more acidic than the pH of the brackish water indicated that pitting was the form of attack in this case. As previously stated, pitting attack of a metal in a chloride-rich environment results in a drop in the pH inside pits versus the pH value of the service medium, i.e., the brackish water in this case. The fact that the concentrations of the detrimental elements – copper, iron and lead - were far below the maximum concentrations permitted by the specification for Al 6061-T6 indicated that this alloy was not defective in composition and thus did not contribute to the severe corrosion that occurred.

In conclusion, it is most probable that the severe pitting corrosion that occurred on this section of aluminum was due to the proximity of the concrete barrier directly above it. Over time, (several years in this case) rain water leached out lime that contained calcium from the traffic barrier above the piling. The resulting rain water and calcium ran down onto the upper portion of the piling. The water evaporated and left behind random deposits of calcium on the aluminum. Chloride ions necessary to combine with the calcium and form $CaCl_2$ were in the atmospheric air around the marina or may have collected on the sheet piling because of the occasional high level splashing of the brackish water during high winds or storms. Like rain water, the brackish water would evaporate and leave behind its chlorides at concentrations much greater than that of the local air. This process could not occur at the other piling section showing minimum, traditional pitting of aluminum because no concrete traffic was there. Instead, there was an aluminum traffic barrier directly above that sheet piling.

The reason the severe corrosion took several years to develop is still uncertain, but two possibilities seem reasonable. The local brackish water had lower chloride content than seawater that was about a mile away at the ocean. The typical chloride concentration of seawater is 20,000 ppm or more, where this brackish water had a content of 14,800 ppm. Thus, the local atmospheric air around the sheet pilings would also have lower chloride content. This would tend to reduce the rate of chloride and calcium interaction on the piling. Secondly, local weather may have been a factor. There may have been more rain storms and windy conditions in recent years than previous years. The more recent extent of splashing of brackish water onto the piling and acceleration of $CaCl_2$ formation would have produced higher corrosion rates than in past years.

The recommendations made may be summarized as follows:

- Hydro blast and then wash off with fresh water the severely corroded piling over its entire length to remove all possible solid corrosion products in and around the pits.
- Weld small circular patches (using only 6061 –T6 material) over all pits that have any significant depth (to assure structural integrity of the piling).
- For long-term minimization of future severe corrosion, bolt a thin plate formed into a projecting “awning” shape onto the outer vertical surface of the concrete barrier over the piling’s length so as to form a barrier above the Al below. Form this “awning” out of Type 316 stainless steel.

Type 316 will offer better corrosion resistance in this marine atmosphere than Type 304 because of its molybdenum content. The formed “awning” should cause most future leaching of lime (and calcium) from the concrete barrier by rain water to run onto its downward slope and fall into the brackish water and not onto the aluminum piling. To prevent galvanic corrosion of the aluminum, the stainless steel should never physically contact the piling.

Case 3 - Copper Fitting Failures in Laboratory Gas Service

A small number of wrought 3/8 X 1/2 -inch copper fittings in a 3/8-inch copper tubing system handling medically pure, inert gases for laboratory use cracked and leaked after being in use for only four months. Several other fittings in the system of the same type had not cracked or leaked. One contractor installed all tubing and fittings. Each fitting was silver soldered to the tubing on one end and had 1/2-inch internal threads on the other end for connection to various screwed-in components needed by the lab. Figure 3 provides a macroscale photo of a typical fitting that leaked.

Figure 3 – Macroscale Photo of a Typical Cracked Copper Fitting Silver-soldered to a 3/8-inch Copper Elbow (the small colored pad is being used to position the fitting for the photo)

The tubing system supplied a mixture of nitrogen and argon gases, or what is known as medical gas. Purity of the delivered gas was essential, so all the fittings were cleaned by a special procedure before installation to remove thread cutting oils and any other residue. The installed tubing and fittings were pressure tested at 200 psi, as the last step in completing the installation. Pure nitrogen gas was used for the pressure test. No system leaks were discovered at the test pressure. Normal operating gas pressure and temperature in the system were 15 psig and 70^0 F.

Initially it was believed that the cracking and leaks may have been produced in the newly installed system by lab personnel that applied too much torque to some of the fittings when they screwed in attachments. Those actions might have created small cracks in the affected fittings, which over a period of several weeks could grow and eventually produce the leaks. To test this idea, the contractor obtained three new fittings of the same type, brand and model number as those that failed but before having the cleaning treatment. They were alternately put in a bench-mounted vise. A ½-inch threaded copper plug was inserted in each fitting. The plug was torqued to a value at least 50% above the maximum recommended level for the fittings. No cracks were found, but each fitting had significant plastic deformation.

The failure analyst was requested to complete a RCFA to find why some of the copper fittings failed while others of the same type, model number and manufacturer did not. Recommendations to correct the problem were also requested.

Investigation of the manufacturing process used for the fittings revealed that they were first compressed (wrought) into shape in dies at ambient temperature, then given a stress relief annealing heat treatment and, finally, bored and tapped to create the internal bore and threads. The wrought process using dies involved compressing a suitable amount of metal between dies shaped to provide the desired final shape of a fitting. The copper alloy used here had more than 84% copper, so it was relatively soft with high ductility. Therefore, comparatively low compressive forces were sufficient to attain the desired solid shape, but internal residual stresses were created. These stresses would add to whatever applied stresses the component might see in service. Accordingly, it was desirable to minimize the residual internal stresses by annealing the parts after the forming process. Stress relief annealing entails heating the part in question to a relatively low temperature, holding it there for a short period and then slowly cooling the part. If the annealing temperature is too high or if the holding period at that temperature is too long, the normal strength of the metal can be significantly reduced. This is because larger microstructural grain sizes can be created during exposures to higher temperatures held for too long.

Two possibilities that seemed most probable to explain the fitting failures were as follows: (1) The normal cleaning procedure, <u>or</u> a mistake made during the cleaning process, caused a form of corrosion in the fittings or (2) some action (or inaction) during the manufacturing steps <u>or</u> during their short time in service had negative effects. Each possibility could have produced the cracks and leaking. One or both possibilities may have acted on some of the fittings while others were not exposed to these harmful effects.

First, the cleaning procedure used was investigated. The installation contractor purchased the copper fittings from a vendor who also did the cleaning. The installation contractor believed that the vendor used phosphoric acid (H_3PO_4) as part of the cleaning process. Research indicated that this acid can cause corrosion of copper in the presence of oxygen. If that acid was actually used, special precautions would have had to been used to prevent corrosive attack during cleaning. However, more investigation indicated that the fittings vendor followed the Compressed Gas Association, Inc. procedure, CGA G-4.1 2004, “Cleaning Equipment for Oxygen Service”. The laboratory owner confirmed this specification was the correct one to use for their medical gas tubing system. It was found that this procedure used hot water, a detergent and perchloroethylene (PERC). None of these items were expected to be corrosive to copper. Therefore, it was anticipated that the cleaning procedure used would have had little or no probability of causing the failures by corrosion. However, that assumption required confirmation.

Possible effects of the manufacturing procedures for the fittings or their exposures during four months of service were evaluated by a series of metallurgical examinations. These were done by evaluating the physical features of one of the typically cracked fittings like the one seen in Figure 3. As is normal in a RCFA, the investigations were approached by progressive steps moving from simple, non-destructive actions to more involved, destructive procedures.

The intact, but cracked fitting was first examined thoroughly at relatively low magnifications with an optical (light) microscope. Here, the objective was to locate obvious secondary cracks, any other surface defects, corrosion or indications of mechanical fatigue. No unusual features were seen in this step, other than the known crack. Next, the fitting was broken open at the crack so as to reveal the fracture surfaces. Without cleaning them, those surfaces were evaluated to identify chemical elements that might be present by using the energy-dispersive x-ray spectrometer (EDS) technique. EDS was part of the scanning electron microscope (SEM) used here. The objective of the EDS exams was to identify any deposited elements that might have produced corrosion or other detrimental effects potentially generated during the compressive forming, stress relief annealing or machining steps during manufacturing or during service. No abnormal deposits were found by the EDS analysis.

Next, the fracture surfaces were cleaned for potentially higher magnification and better resolution examinations in a SEM. These evaluations were intended to provide more detailed information on the possible presence of secondary cracks, fatigue or some form of corrosion such as general attack, pitting or stress-corrosion cracking. The SEM views of the fracture surfaces would also indicate whether the known crack was produced by ductile or by brittle fracture. Establishing the fracture mode might indicate whether negative material properties that led to the leaks may have been created during steps in the manufacturing process.

Figure 4 is a photomicrograph of the fracture surface of the crack, after cleaning, taken while the broken-apart fitting was in the SEM. The internal threads of the fitting were apparent just below the fracture surface at this low 10X magnification. The red boxes represent areas on the fracture surface that were later examined separately at higher magnifications to possibly reveal more details. No evidence of secondary cracks, any form of corrosion or fatigue was seen in any of the SEM examinations. The key finding seen in Figure 4 and confirmed by viewing each of the three boxed areas on the surface, was the smooth texture and appearance of the fracture surface. This indicated that the fracture was brittle. That is unusual because copper typically is soft and ductile and thus it normally fractures in a ductile manner.

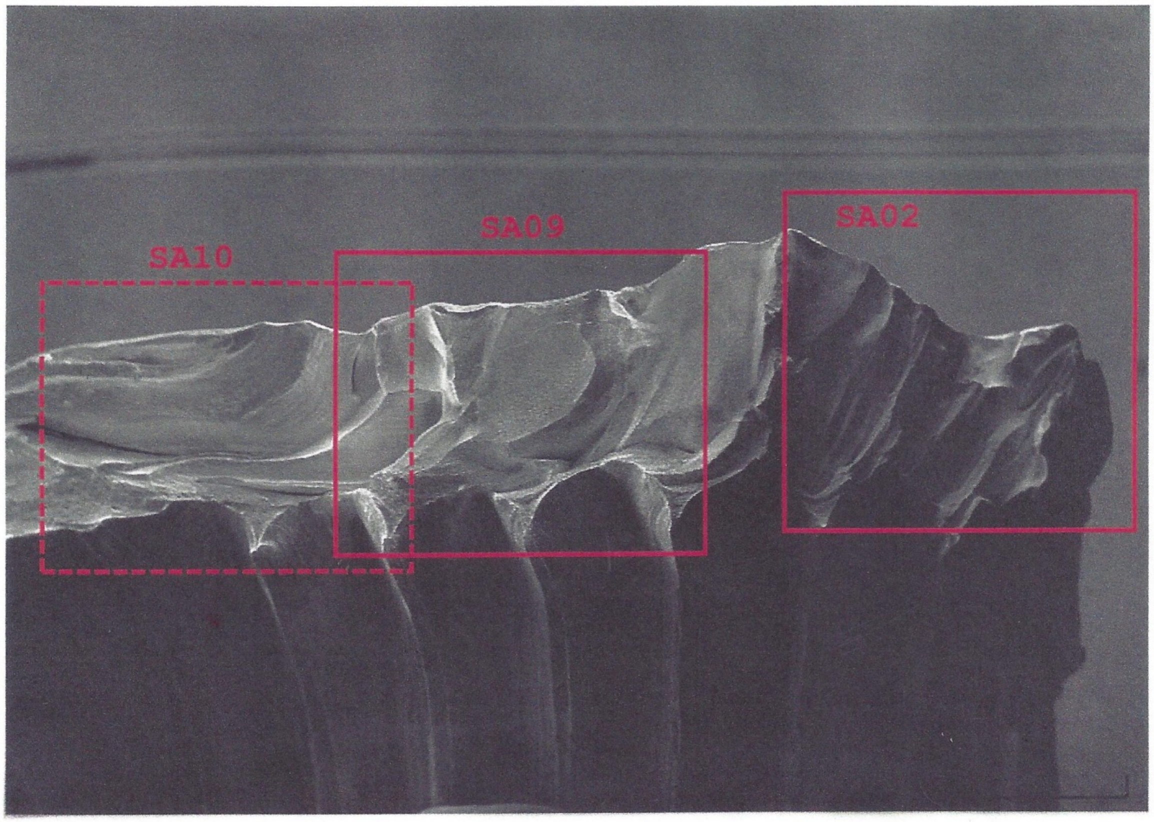

Figure 4 – SEM View of Brittle Fracture Surface of the Broken-apart Copper Fitting at 10X Magnification. Boxed Areas Were Later Examined at Higher Magnifications.

For comparison to Figure 4, the SEM photomicrograph in Figure 5 is from another source and is not part of the present case. It is a fracture surface of a copper component showing the normal ductile surface appearance most common for copper. The surface is not smooth like the brittle fracture in Figure 4. Instead, it has a series of uneven dimples that are characteristic of ductile fracture in many metals. Different magnifications will indicate different sizes of the dimples seen.

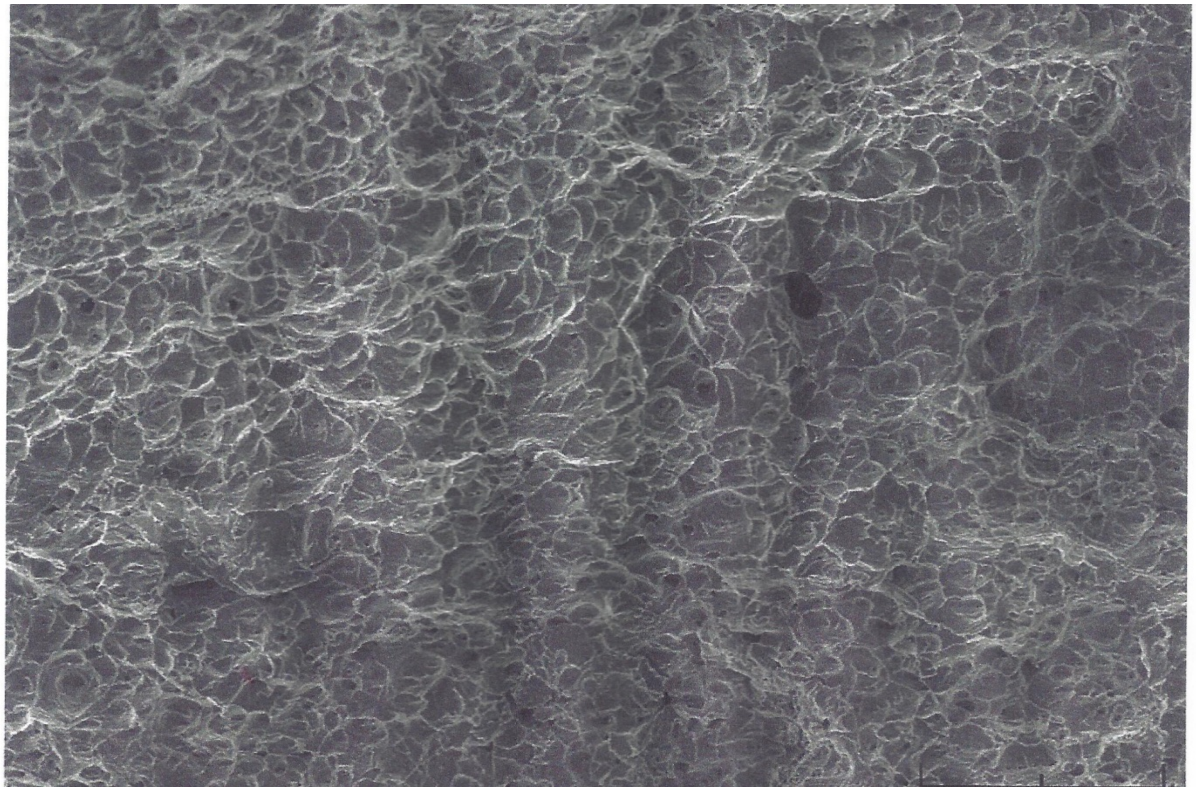

Figure 5 – SEM Photomicrograph of the Typical, Dimpled Ductile Fracture Surface of Copper. This Copper Was Not Part of Case 3. 250X Magnification.

It was desired to examine the microstructure of the failed fitting for evidence to explain the brittle fracture mode. To do this one half of the broken-apart cracked section was saw-cut through the metal perpendicular to the path of the crack. This provided a flat cross-section of the metal perpendicular to the crack that was then cast in a resin metallographic mounting. The exposed cross-sectional surface was polished and etched to preferentially corrode the grain boundaries and thus reveal grain sizes in the metal. The resulting mounting was examined in a light microscope. Figure 6 is a photo of the polished and etched mounted surface at low magnification. The outside diameter of the fitting, i.e., the top edge of the opened crack, is the top of the cross-section, while the bottom edge is the bottom of the crack near the fitting's inside diameter.

The most significant finding was the extremely large sizes of the grains as indicated by the visible grain boundaries. Few grains and grain boundaries are seen because the corrosive etchant could only preferentially attack the grain boundaries around those portions of the large three-dimensional grains that penetrated the polished cross-sectional plane examined. In addition, apparently, the etchant did not contact the available grain boundaries in this plane equally, so some are more distinct than others.

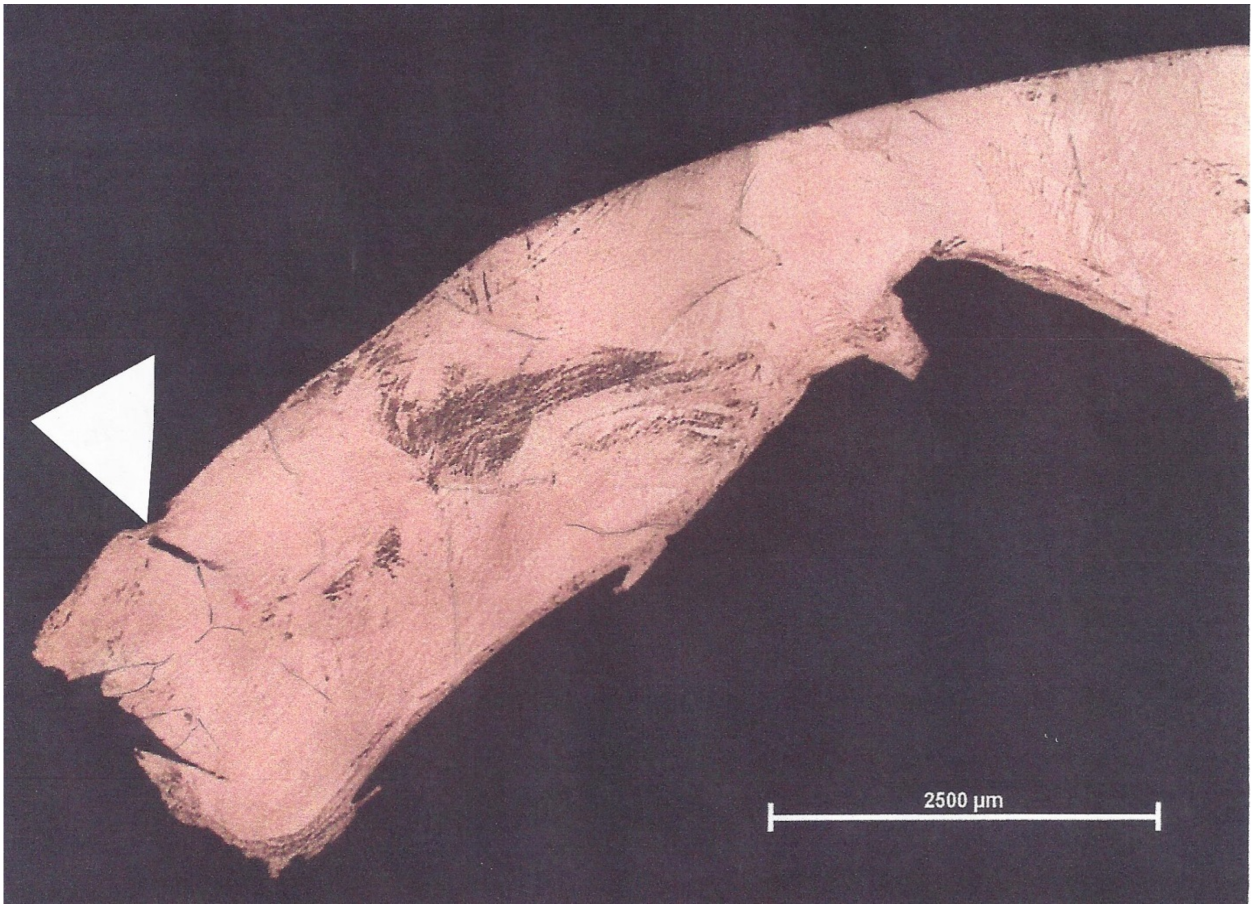

Figure 6 – Light Microscope Photo of a Polished and Etched Cross-section Through the Copper Fitting's Fracture Perpendicular to the Crack Path. 12.5X magnification.

The white triangle attached to the photo points to a dark oblong-shaped feature at the crack opening on the outside diameter of the fitting. This an open secondary crack, in the examined plane, coming off the main crack. Just below and joining the secondary crack is a grain boundary that has increased width. This grain boundary is wider because it has an intergranular crack that is growing through it towards the intersection of three large grains. Other less clear examples of intergranular cracking were also seen. Intergranular cracking in the fitting was significant because this type of cracking often occurs when large grains are present. Additional examinations were completed with this cross-section at higher magnifications but still using a light microscope. Nothing more was learned. Many of the discontinuous grain boundaries and intergranular secondary cracks were simply seen in more detail.

A summary of the conclusions from this RCFA is as follows:

- The failed copper fittings developed small cracks that eventually grew enough to penetrated the fittings and produce the gas leaks.
- Incorrect stress relief annealing heat treatment caused the failures. Specifically, the deficient annealing process involved either a holding temperature that was too high, a holding period that was too long or both.
- This resulted in the large grain sizes that significantly weakened the copper. Brittle fracture is often associated with large grain sizes and with it intergranular cracking.
- No form of corrosion, mechanical fatigue or other reason was shown to have had a role in these failures.
- It is likely that the failed fittings developed small internal cracks initially during the 200 psig pressure test by the contractor. However, the service pressure and temperature were so low (15 psig and ambient) that the original cracks took a few months to penetrate the wall thickness of the fittings.

Not all the copper fittings in the medical gas tubing system failed this way, because these small fittings are stress relief annealed in batches. Apparently, proper conditions for annealing were not in effect for the batch that included the failed fittings, and that was likely an aberration in operations by the manufacturer. Other projects may have unknowingly used fittings from this defective fitting batch , while properly treated fittings from another normal batch were simultaneously installed in the present tubing system.

Corrections of the fittings in this medical gas system have been completed, which consisted of replacing the leaking fittings. Consideration should have also been given to removing two or three of these replacements early in their service lives. The removed fittings could then be sectioned, polished and etched as metallographic mountings. These could then be examined to confirm normal grain sizes and thus proper annealing stress relief treatment of the copper. The contractor for this installation likely had unused fittings from the same fittings vendor as used in this project and thus might well have considered the same precaution.

Case 4 - Failure of a Critical Bolt on a Child's Backyard Swing

A young girl suffered two broken ribs and a twisted ankle when she fell from her backyard swing. One of the two steel eye bolts fractured that had supported one side of the swing seat from a wooden beam. The parents purchased the swing hardware as a packaged set from one manufacturer. The father built the swing's wooden frame using the proper grade and sizes of components as provided in the hardware manufacturer's instructions. No wooden parts of the swing failed in the accident. A key aspect of the bolt failure was that the incident occurred only twelve days after the father installed the swing. The injured child and other neighborhood children had used it during that time. She was of normal weight and size for her age of ten.

Figure 6 provides a sketch of the general assembly of the suspension components for the swing near the wooden beam. When assembled with the lock nut tightened, the outer top edge of the eye of the bolt just touched the bottom surface of the beam. As indicated, the fracture of the installed bolt occurred very near the bottom of the beam in the lowest threads of the eye bolt.

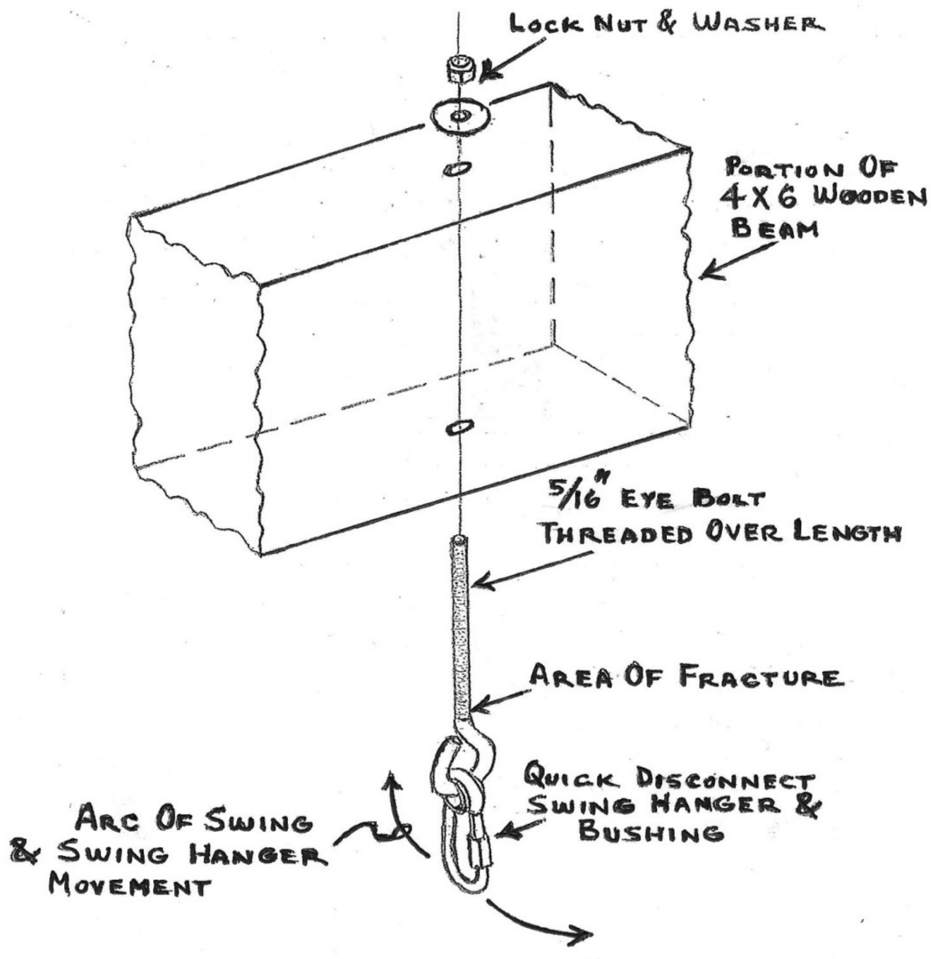

Figure 7 – General Assembly of the Swing's Components Near the Area of Fracture

The failure analyst was requested to determine why the eye bolt failed and caused the accident. The belief was that the bolt may have failed by fatigue, but the major problem with that assumption was why the fracture would occur after only twelve days.

Some alternative failure mechanisms that were evaluated included the following: Improper assembly of the swing, unintended use – such as one or two uses by an adult that initiated a crack in the bolt that grew rapidly, fatigue acting in conjunction with poor properties of the steel bolt or poor design. Each alternative was investigated.

First, the instructions provided by the hardware manufacturer for building this wooden A-frame swing structure with the hardware were thoroughly reviewed. Then, without showing him the instructions, the father that built the A-frame and installed the hardware was interviewed and asked several open-ended questions specifically about the construction and assembly. He was asked for more details whenever his response was, "I just followed the instructions", while being careful to avoid accusations of wrong-doing. This interview convinced the failure analyst that the father had, in fact, utilized good carpentry and mechanical practices to build and assemble the swing set using the given instructions.

Next the possibility of unintended use was investigated by talking separately with the child's mother. This took place as part of the first on-site inspection of the swing while most of the fractured bolt was still in the beam. Again, being careful to avoid accusations, the analyst asked some general questions. For example,

- Did any of the neighborhood friends of her daughter use the swing?
- Were any of them much older and heavier than her daughter?
- Did she witness any of the kids swinging in a wild or destructive way?
- Did visiting parents ever sit and move in the swing while their child was playing with her daughter in the backyard?

After carefully considering the mother's reactions to these questions the analyst concluded that improper use of the swing was not a probable cause of the failure.

The bottom and top portions of the fractured bolt were recovered at the accident site. The fracture occurred in the threaded portion and specifically in the first two or three threads above the eye of the bolt very near to the bolt's original contact point with the bottom of the beam as seen in Figure 7. Both portions of the bolt had what appeared to be a galvanized coating. A review of the hardware manufacturer's on-line sales literature later confirmed this. The galvanizing in the threaded portion of the bolt, i.e., over most of its total length, appeared relatively rough and uneven. The fractured area had only a small amount of plastic deformation of the metal. The deformed area seemed to be near the center of each fracture surface.

The fracture surfaces on the two portions of the bolt were examined in more detail, first in a light microscope and then in a SEM. Photomicrographs were made of these surfaces while in the SEM, but unfortunately, those were lost before this writing. However, Figure 8 is a sketch which provides the salient features of both fracture surfaces as seen in the SEM at low magnification. Those examinations confirmed that the bolt experienced fatigue loading. Two fatigue cracks initiated and grew,180 degrees apart, from two areas on the outside surface of the bolt in the threads. Each time the swing moved back and forth, the bolt received a reverse bending fatigue cycle. The two fatigue cracks grew towards the center of the bolt until too little sound metal remained in the bolt to support the applied forces. The final fracture was by stress overload.

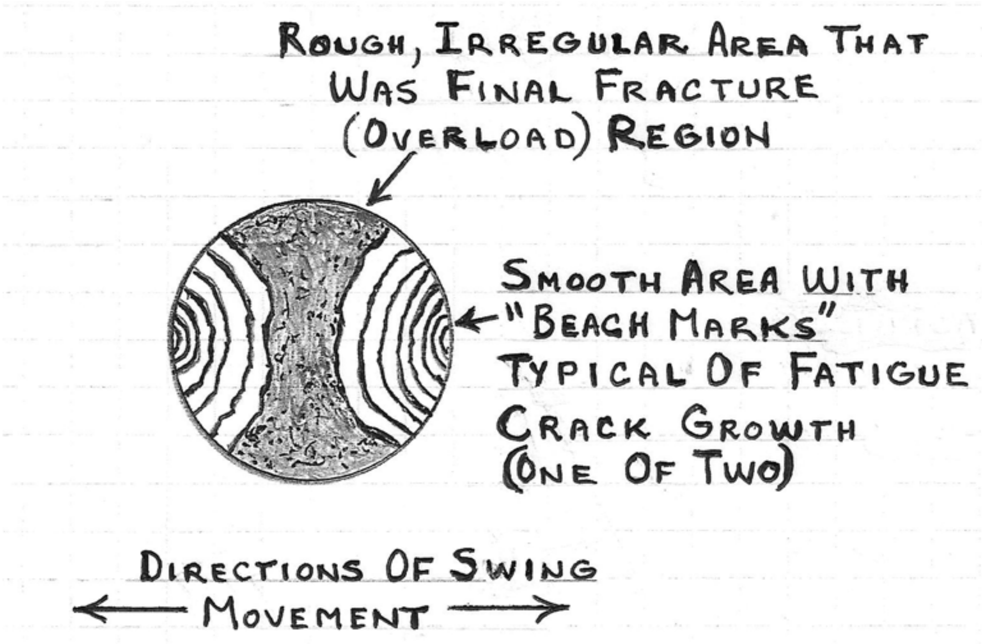

Figure 8 – A Representation of the Cross-section of the Fracture Surface of the Eye Bolt as Seen in a SEM at 50X Magnification. (Descriptive notes have been added).

Explanation for the very rapid fatigue failure was sought by evaluating the mechanical and metallurgical properties of the bolt. The hardware manufacturer's literature indicated the supplied bolts met the ASTM Standard Specification A307 for Grade A material. This specification provides information on acceptable values of chemical composition of the steel, ultimate tensile strength (UTS) and percentage elongation. There was sufficient material to complete a composition analysis with the optical emission spectroscopy (OES) technique, so that less expensive analysis method was used. The A307 spec defined acceptable percentages of carbon, phosphorus, sulfur and manganese in the steel. The OES analysis showed the bolt material met all the composition requirements of A307.

Tensile test specimens were made from the available bolt material and tensile tests of those specimens were completed as per the ASTM E8 standard. The tests indicated both the steel's UTS and its percentage elongation. The UTS value was considerably above the minimum value required by A307. However, the measured percentage elongation was only about half of the minimum value required by A307. Percentage elongation is a direct indicator of a material's ductility, so the ductility of this steel was deficient based on the specification. UTS and ductility are normally inversely proportional. Therefore, it is normal that the measured UTS was much higher than the minimum required by A307 due to its low ductility.

A cross section of the failed bolt was prepared as a mounted metallographic specimen, then polished and etched to reveal the microstructure and grain sizes plus other features . The sample was examined in a light microscope. In general, the microstructure was normal for the low-carbon content steel that was used for the bolt. Grain sizes were clearly abnormal. ASTM Test Method E-112 was used to measure the average grain sizes in the cross section. E-112 defines a total range of grain sizes from 00 (the largest) down to 14 (the smallest). The average range of the size of grains in this steel was 9.0 to 9.5. These are very small grains. This finding agreed with the measured mechanical property values of high UTS and low ductility. Smaller grain sizes produce higher UTS values but lower ductility values.

Both a material's strength and its ductility affect its resistance to failure by fatigue. It is optimal to have both high strength and high ductility to attain the best fatigue resistance. Of course, this is difficult to achieve because these two properties are inversely proportional. A bolt's manufacturing process is critical to both its final mechanical and metallurgical properties .

The common sequence used to produce round rods from which bolts of this type are made begins by drawing, i.e., pulling, smooth larger diameter steel rod material through a closed, circular die (or series of dies) to achieve the desired diameter. This is done before threads are rolled onto the surface of the reduced-diameter rods. The drawing process plastically deforms, or "works", the steel, which increases its strength because of the significantly reduced sizes of grains, but ductility is also reduced. After drawing, there is an important annealing heat treatment step. The annealing must be closely controlled to achieve the best trade-off between strength and ductility. Here, grain growth by annealing was desirable in the worked, drawn rod material to regain some degree of ductility, but excessive grain growth decreases strength significantly. The very small average grain sizes found in this failed bolt material indicated it did not receive a proper annealing treatment, which resulted in the very small grains and deficient ductility. Final steps in manufacturing were to form the eye of the rods, roll threads onto the rods and provide the galvanized coatings.

Additional notable features of the failed bolt were seen on the outer edge of another prepared (polished and then etched) metallographic cross-section sample, directly at the outer edge of the fracture surface. These were metallurgical laps. They are seen most clearly in Figure 9 in the top photomicrograph before the sample was etched and less distinctly after etching in the bottom view. The lower view also shows the very small grain sizes of this steel. Both were originally viewed at 100X magnification.

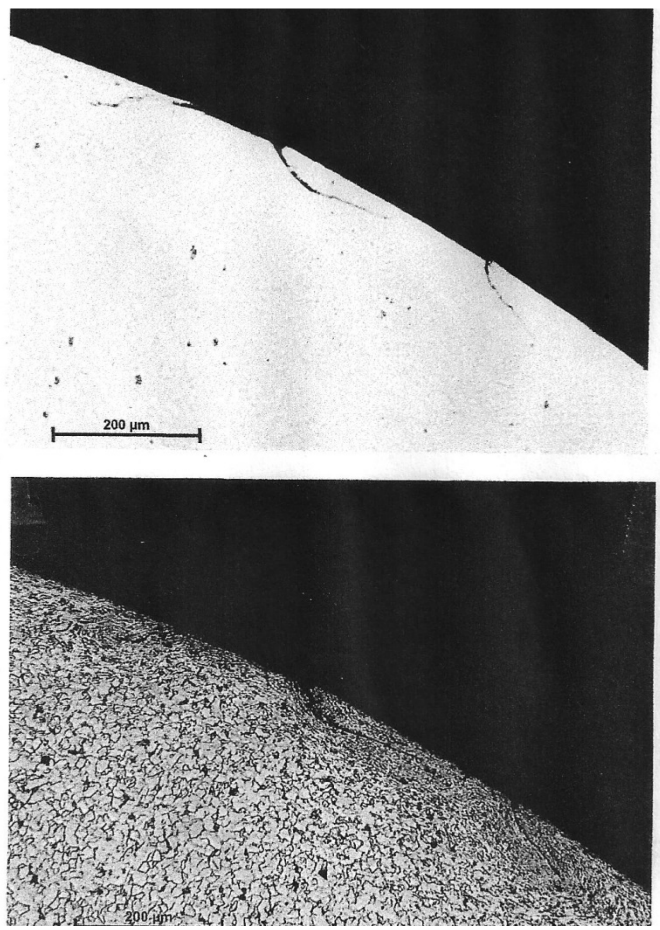

Figure 9 – Photomicrographs of a Prepared Metallographic Cross-section at the Outer Edge of the Bolt's Fracture Surface Showing Laps. Top Photo is Before Etching and Bottom Photo is After Etching. Both at 100X Magnification.

Laps are micro-scale fold overs of metal at the surface with varying extents of penetration into the metal. Small surface defects are created and these can act as stress concentration points that lower resistance to the initiation of fatigue. In this case, they likely also contributed to the generally rough and irregular macro-scale appearance of the zinc coating initially seen on the galvanized surface of the failed bolt.

Laps are created on a formerly smooth metal surface as a result of certain deficiencies that can occur during the mechanical rolling manufacturing step used to generate threads. If done perfectly and no laps are created, rolled threads offer better fatigue resistance than machined threads. Rolling is also less expensive to accomplish than machining. The ASTM Standard, F788, Specification for Surface Discontinuities of Bolts, Screws and Studs defines acceptable limits on the length and extent of penetration of laps that may occur with rolled threads. The laps found here and seen in Figure 9 were very close to, but still below, the size defined as prohibited for fasteners in dynamic stress service, i.e., fatigue loading, as stated in F788. However, it was reasonable to assume that these laps were at least contributing factors in the very short fatigue life of the failed bolt.

The final area investigated as a possible cause of this failure was the general configuration or design of the bolt as supplied by the hardware manufacturer. As shown in Figure 7, the supplied bolt was threaded over most of its straight length. This was not required or desirable. The threaded section could have been confined to only the top portion of the bolt so as to allow engagement with the lock nut on the top of the beam. Many mechanical engineering design references make the point that threaded portions of stressed components act as stress risers. They concentrate and increase any applied stress beyond the level in non-threaded sections by a factor that varies with the specific type of threads. This effect is especially important when the applied stress is dynamic, i.e., fatigue loading.

In this case, the bottom threaded portion of the bolt was at a position very near the point of maximum back and forth bending forces that alternately produced tensile and compressive stresses on the two bolt edges. The proximity of the lower threads unnecessarily magnified these stresses. That stress concentration effect could have been significantly decreased or eliminated if the first bolt threads were far inside the hole of the wooden beam near its top. This design (or hardware supplied mistake) decision was judged to be an important contributor to the failure.

In conclusion, this bolt failed by greatly accelerated fatigue because of the joint effects of two interacting classes of factors as follows:

- Deficiently low ductility of the steel likely due to an inadequate annealing process after the drawing step during manufacture of the bolt, resulting in very small metallurgical grain sizes that compromised a trade-off between strength and ductility for optimal fatigue resistance.
- Applied stress concentration caused by the marginally acceptable lap sizes, unnecessary use of threads over the full length of the bolt and the generally rough surface condition of the galvanized coating

It is uncertain which of these contributing factors to the failure was most important. This history involved a legal case (details not discussed here), so the failure analyst was not asked for recommendations for corrective actions.

Case 5 – Grooving Corrosion of Carbon Steel Pipe Used for Pilings

Several welded steel pipes serving as pilings to support a dock-side platform in a harbor had not yet failed but had various extents of localized corrosion confined to their longitudinal welds. Some spots of corrosion penetrated as much as half of the 0.5-inch pipe wall thickness. The form of corrosion is known as grooving attack. The longitudinal welds were made by the electric resistance welding (ERW) process and completed by the manufacturer of the pipe. The nominal diameter of the pipe was 14-inches. All the pilings were installed and had been in service at the harbor site at least thirty years since their manufacture in 1970. Recent underwater inspections found the grooving corrosion. Initial installation of cathodic protection (CP) controlled corrosion of the pilings, but in recent years, its operation was uncertain. Figure 10 is an approximate cross-sectional representation of one of the many installed pilings.

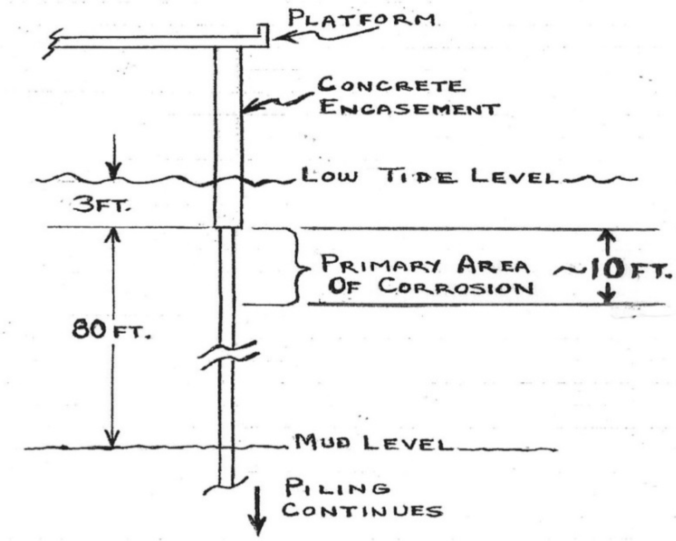

Figure 10 – Cross-sectional Configuration of an Installed Pipe Piling

It was fortunate that the engineers that specified encasement of the piling supports also knew that, in most waters, the most severe corrosion on vertically installed steel occurs in the splash zone, just above and slightly below the low water level. This is because oxygen from the air is most readily available to the wetted steel in these areas. Because concrete encased those areas of the piling, the substrate steel there was protected from corrosion. Oxygen is necessary to promote the common cathodic reaction in aqueous corrosion, i.e., the electrochemical reduction of oxygen to yield hydroxide ions. Easily available oxygen accelerates the cathodic corrosion reaction. Since the anodic and cathodic reactions must occur at the same rate, the overall rate of corrosion then increases. It was also most fortunate that this harbor water was brackish with a lower chloride content and, therefore, less corrosive than open seawater.

The amount of dissolved oxygen in the water decreases as distance below the free water surface increases. Therefore, it is not unusual that the variable amounts of grooving corrosion were found just below the concrete and relatively close to the water surface as shown in Figure 10.

The failure analyst was requested to complete a RCFA to determine why this specific form of corrosion had occurred, especially only after the long-time service of the pilings, and what corrective measures should now be implemented.

The following possible causes for the corrosion were investigated:

- Factors important in causing grooving corrosion in ERW formed steel pipe.
- The chemical composition and microstructure of the steel used for the pilings.
- The type and history of the CP used for the pilings.

Research in corrosion literature sources indicated that grooving corrosion of older ERW steel pipe in both seawater and in underground pipeline service was relatively common. However, conditions at the harbor were estimated to be less aggressive. Generally, grooving occurred in ERW pipe made before about 1978. It was seen that parameters used in the ERW manufacturing process and the composition of the steel contributed to the early susceptibility.

Typically, ERW pipe manufacture begins with a narrow 20 to 30-foot rectangular length of rolled steel plate that is hot formed into the desired diameter by bending it around its longitudinal center axis and forming a pipe shape. Then a large force is applied to push the two touching plate edges together while an AC electric current is simultaneously passed through the joint to create a resistance weld. The AC current used before about 1978 was low frequency. Since that time, high frequency AC has been used. This frequency change plus strict control on the composition of the steel, particularly minimizing the amount of sulfur permitted, greatly decreased the incidents of ERW grooving corrosion. The final step in the manufacturing process has always been (and continues) to complete a post-weld heat treatment to minimize residual stresses and reduce steel hardness produced by welding. This lessens susceptibility to environmental cracking processes such as stress-corrosion cracking or hydrogen embrittlement.

All common steels contain manganese, and the older versions of ERW pipe also contained significant amounts of sulfur. When such a composition exists, inclusions of manganese sulfides (MnS) often form in the steel. These inclusions are particularly susceptible to corrosion. Increased sulfur content can be detrimental even when MnS inclusions don't form. In addition, the microstructure of any type of arc weld is inherently non-homogeneous, i.e., the microstructures of the parent metal, the heat affected zone (HAZ) and the fusion area are all different. This is important to the extent of corrosion that may occur. A generally homogeneous microstructure maximizes corrosion resistance in a metal, welded or not . A non-homogeneous structure decreases resistance. That's why pure metals are generally more corrosion resistant than alloys even though alloys are needed to provide practical mechanical properties.

A diver using a small hole saw collected samples from corroded ERW joints in the pipe pilings . These were used to define the composition of the steel and to prepare metallographic mountings that were polished and etched. The mountings were used to evaluate the microstructure of the steel in and immediately around the corroded ERW joints. Multiple photomicrographs of the mounts were made while they were being examined in a light microscope. The energy-dispersive x-ray spectrometry (EDS) technique defined the primary chemical elements present in the steel and their relative amounts.

The EDS analyses showed that the steel had high sulfur contents. Current practice for ERW pipe is to maintain low sulfur levels and to add small amounts of copper and chromium. The latter two elements counteract the negative effects of sulfur on corrosion resistance. Analysis of the corroded steel samples indicated that no copper or chromium was present.

Figure 11 is an etched metallographic cross-section of the pipe wall through the ERW joint showing severe grooving corrosion at low magnification. Penetration here is about 40% of the wall thickness. Figure 12 is a somewhat higher magnification montage (two photos) of the same groove showing three distinct areas indicating the non-homogeneous microstructure of the weld area. The outer, somewhat lighter, areas are parent metal, the slightly darker area immediately on each side of the open groove are heat affected zones (HAZ), and the almost all white, but irregular strip down below the bottom of the groove, is another region that has not yet corroded with a still different appearance. Figure 12 illustrates typical non-homogenous microstructures in welds that make them more likely to experience accelerated corrosion rates compared to the rates of attack on parent metal.

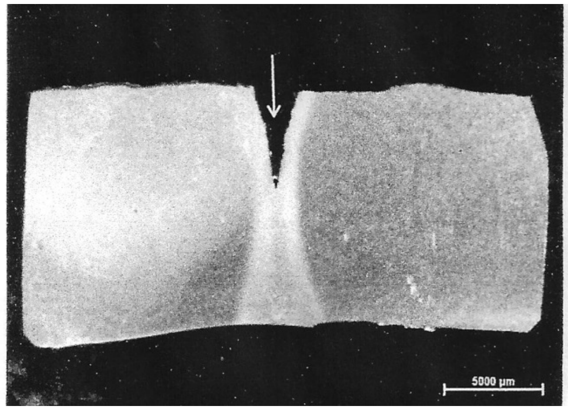

Figure 11 – Cross Section of the ERW Pipe Wall Showing Severe Grooving Corrosion at the Center of the Weld. Magnification 5X.

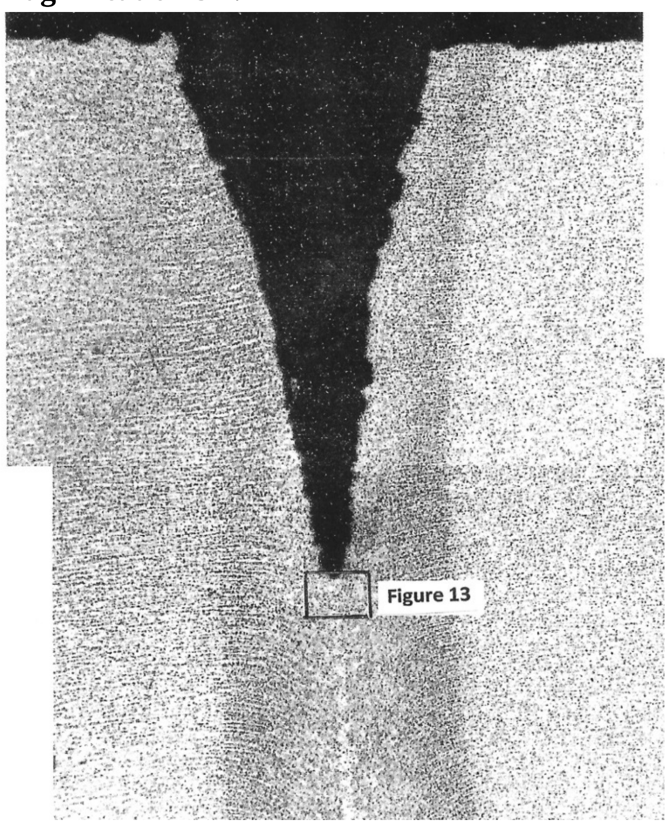

Figure 12 – Same Cross Section of Groove Corrosion as Seen in Figure 11 Illustrating Three Distinctly Different Metallographic Appearances. Magnifications 15X.

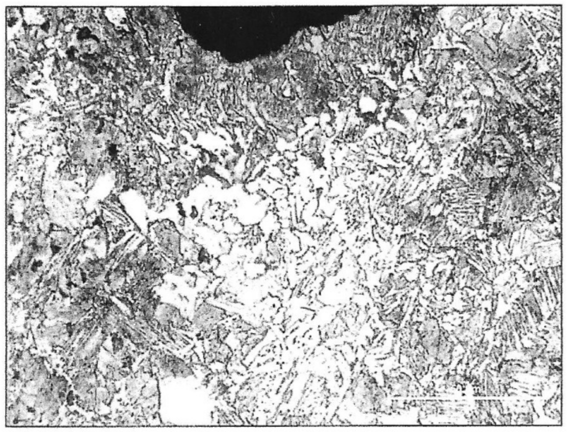

Figure 13 – Higher Magnification View of the Bottom, Tip Area of the Corrosion Groove Shown in the Box of Figure 12. Magnification 500X.

Figure 13 is a photomicrograph of the boxed area seen in Figure 12 at increased magnification. This region did not show any linear manganese sulfide inclusions that are often seen in steel with high sulfur content, although the EDS analysis confirmed high sulfur content in this steel. The high percentage of sulfur was a clear harmful factor in accelerating corrosion. The centerline of the weld contained a higher concentration of ferrite (white phase that is void of carbon) than the surrounding HAZ that is a mixture of ferrite and various heat transformation products that contain carbon (white and dark phases). Exposures to different temperatures during the overall ERW process created the mixed microstructure areas.

A thorough evaluation of the history of the use and verification of cathodic protection (CP) on the pipe piling was completed. According to records, a sacrificial-anode type of CP was initially installed on the piles below the level of the concrete encasements. After installation and for about the first fifteen years of service, readings of the electrochemical potentials of the steel were made annually to assure that a protected status existed. That was confirmed by examination of monitoring CP records that had been filed away. However, during the more recent years, the periods between monitoring began to lengthen until no monitoring was accomplished for a few years, before the current variable corrosion was found. The change in practice generally overlapped with a change in responsible management personnel.

It is well known that sacrificial CP anodes do not typically provide sufficient current output to provide protection beyond about twenty years of use. It was very favorable that this water was brackish and, therefore, less corrosive compared to seawater. It was also fortunate that the corroded steel was not in the splash zone and below the low tide water level, thus there was less available oxygen to support corrosion. Consequently, the rate of grooving corrosion was less than it would have otherwise been in recent years with little or no CP current being delivered.

Variable extents of grooving corrosion occurred on the lower portions of these pilings because of multiple contributing factors. Conclusions were as follows:

- These were old vintage ERW pipes, i.e., those produced prior to about 1978, and were welded using a low frequency AC resistance welding process that is now known to often cause susceptibility to this form of corrosion.
- In addition, analysis showed that the sulfur content of this steel was high – much higher than current practice allows in ERW pipe and that created a distinct susceptibility to grooving attack.
- As a general rule, welds are more susceptible to several forms of corrosion because of the non-homogeneous nature of their microstructures. It was shown that these ERW welds had that characteristic.
- Finally, useful CP was initially applied and regularly maintained on the pilings but in recent years that had not been done.
-

Brackish harbor water and the reduced availability of oxygen at the depth of the non-encased pipe were important factors that likely helped to minimize the variable corrosion that might have otherwise occurred.

Recommendations included the following:

- By means of inspections, define the areas on the ERW joints of all the pilings that have corrosion grooves that penetrated the pipe's wall thickness by 25% or more and weld on low-sulfur content carbon steel patches at those points.
- Re-install a sacrificial anode CP system for all the pilings, designed and installed by a contractor that is knowledgeable in CP of carbon steel in brackish water.
- Understand that, at a minimum, a CP system must continue to be monitored annually by competent CP personnel for adequate protection, and that sacrificial anodes must be replaced when they can no longer provide sufficient current output to provide protective electrical potentials on the steel.

Case 6 – Failure of a Large Crude Oil Storage Tank

Note: This case is a summary of an earlier RCFA completed by Dr. Iain LeMay and his organization, Metallurgical Consulting Services Ltd. in Saskatchewan, Canada. The work was described in his August 1982 article in ASM International's *Metal Progress* entitled, "Failure Analysis of a Crude Oil Storage Tank". Use of that source is gratefully acknowledged.

During the night of December 1, 1980, a welded 100,000 barrel fuel oil storage tank experienced a catastrophic structural rupture, resulting in an explosion and a very large fire. This occurred in Moose Jaw, Saskatchewan, Canada. The steel tank had been constructed in 1952 and was essentially full of oil at the time of the failure. Apparently, explosion of the air-vapor mix in the tank ignited oil escaping through the opening and led to the fire. There were no injuries, but there was extensive property damage over a large area of Moose Jaw. The explosion caused major portions of the tank walls and roof to be blown apart and thrown onto and beyond the surrounding concrete containment dike.

The failure originated at the welded manway and reinforcing pad on the bottom, vertical section of the tank. The major vertical rupture occurred as shown, schematically, in Figure 14.

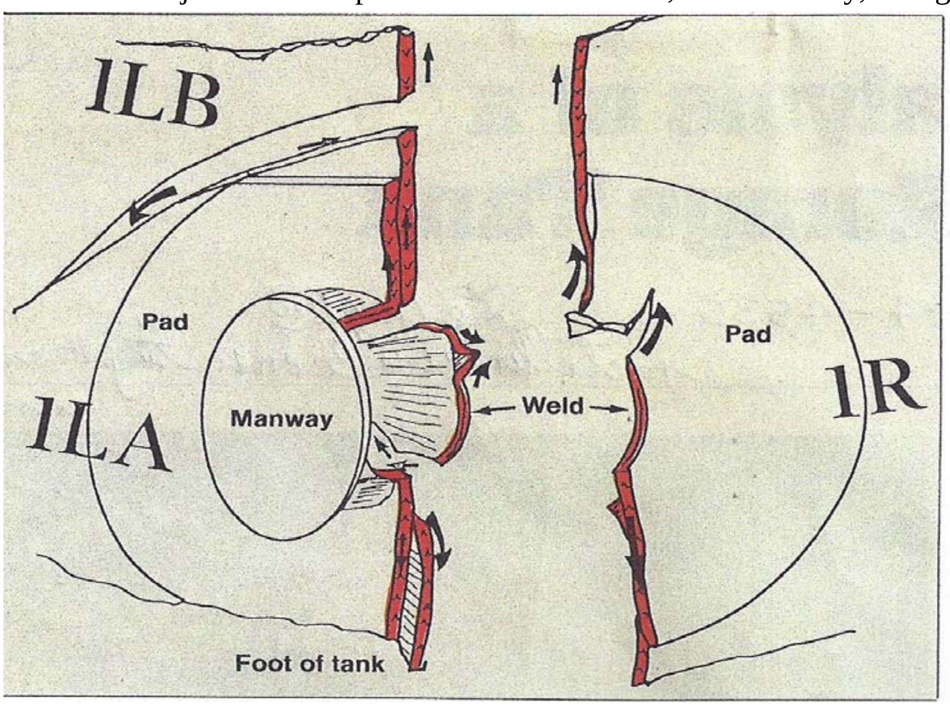

Figure 14 – Fracture Surfaces At and Around the Tank Manway.

The initial site visit showed there was little plastic deformation of the steel in the manway area, which indicated brittle fracture of the material. The blown apart wall and roof plates were located approximately 180 degrees from the manway on the tank's circumference. Black arrows in

Figure 14 indicate the direction and paths of crack growth, while the small chevron markings on the fracture surfaces point towards the origin of the cracks. That evidence confirmed that the rupture originated from the circular weld that joined the neck of the manway to the reinforcing pad. Three sections of fractured plate were removed from the site and identified, as shown in the figure, for later examinations.

The failure analyst was requested to determine the cause of the tank rupture. The following potential issues were investigated: the steel's chemical composition, metallurgical properties and mechanical properties; the quality of the manway neck weld; possible abnormal stress levels that may have been present in the tank.

The specified steel used for the tank was ASTM A283. Analysis showed the composition of the failed steel generally met the composition requirements of A283. However, the ratio of manganese-to-carbon present was very low at 2.17. This low value would make the steel more susceptible to brittle, fast fracture. Even prior to the construction of the tank in 1952, it was known that resistance to brittle fracture at low temperatures required steel with a Mn-to-C ratio of at least 3.0. The current specification for A283 requires nominal amounts of Mn at 0.9 % and C at 0.24% to provide a Mn-to-C ratio of 3.75.

Evaluation of the microstructure of the material required the completion of metallographic examinations of multiple samples of the steel. These evaluations indicated the material properties were generally normal for this low carbon steel plate that had been hot rolled during manufacturing. However, indication that the steel had been exposed to temperatures of 930^0 F to 1200^0 F during the fire was evident due to some spheroidization of the carbide within the pearlite. No ferrite grain growth was observed. The findings suggested the fire affected certain material properties. Strength would have been slightly reduced, while ductility would slightly increase because of reduction of residual manufacturing stresses. The steel's ductile-to-brittle transition temperature (DBTT) would also have been slightly decreased because of exposure to the heat. These effects of the fire, acting <u>after</u> the steel ruptured, were considered when assessing measured values of mechanical properties of the material recovered from the failure site.

Mechanical tensile tests of the steel samples were completed in accordance with the standard ASTM Test Method E8 to define the steel's yield strength, ultimate tensile strength and percentage elongation. The latter indicates ductility. The post-failure steel test specimens still met all three of these specified requirements for A283 steel.

Susceptibility to brittle fracture of steels at low temperatures, i.e., their ductile-to-brittle transition temperature (DBTT), cannot be predicted by the values measured in a standard tensile test. Instead, DBTT values of both reinforcing pad and tank shell materials were determined in Charpy V-notch tests. Test specimens were machined and tested in accordance with the ASTM Standard Test Method E23 and evaluated over a range of test temperatures. The impact energy criterion of 15 ft-lbs (23.3 Joules) for defining a generally accepted value of DBTT for low-strength carbon steels was used. Impact energies below this criterion indicate brittle fracture is likely and energies above it indicate ductile fracture is probable. Figure 15 shows the plotted, mean values of generated test data.

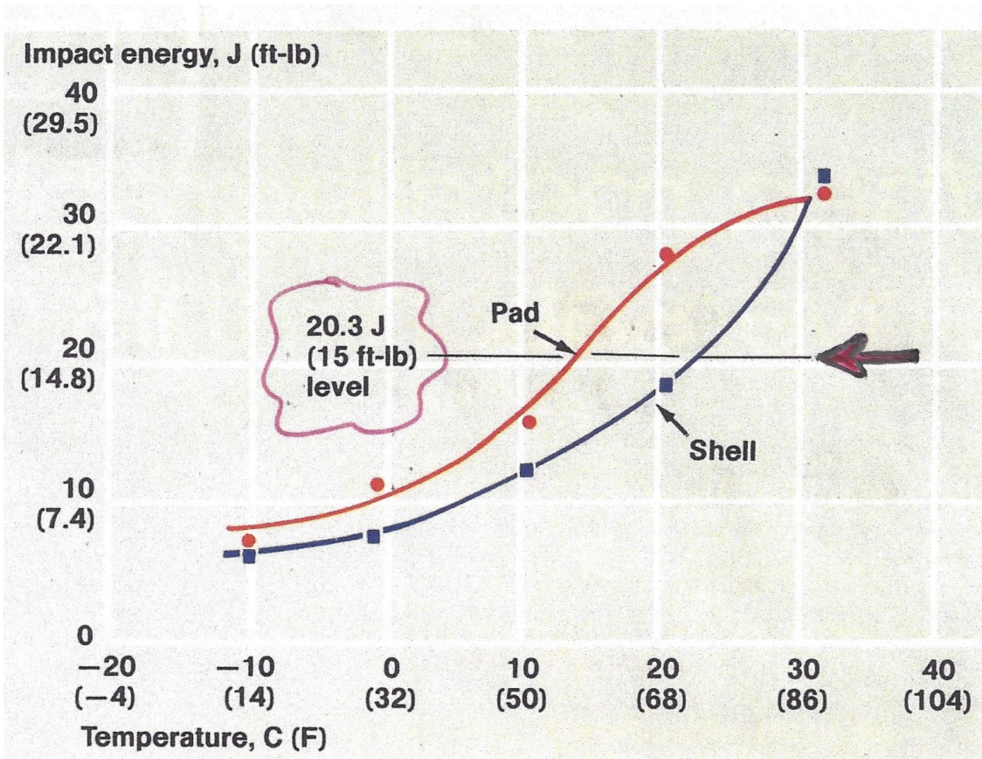

Figure 15 - Charpy V-notch Impact Energy Data Used to Define DBTT Values of the Tank's Steel at the Reinforcing Pad and Shell Plates

The data indicated that the DBTT's for the pad and shell steel in the tank were approximately 57 and 72 degrees F, respectively, at the 15 ft-lb energy level. Both values are extremely high and indicate there would be no resistance to brittle fracture at normally expected winter temperatures in this location. Investigation indicated that, during the night of the failure, the ambient air temperature was approximately -17^0 F after a daytime value of approximately 29^0 F. The oil in the tank was estimated to be in the range of 37^0 to 26^0 F. Brittle crack initiation and growth in steel in the pad and the shell were essentially unavoidable given these conditions.

The ground temperature under the steel plates in the base of the tank was expected to remain at about the same temperature as the oil inside. Thus, when the air temperature and vertical walls of the tank dropped significantly below that higher temperature of the tank base, the contraction of the base would be expected to be minimal. This difference would induce bending stresses in the area of the manway and all lower sections of the tank walls.

Prepared metallographic cross-section specimens through intact portions of the generally fractured weld between the manway neck and the pad were examined. Incomplete penetration of the lower portion of this single bevel groove weld was clearly seen. At higher magnification, small cracks in the weld could be seen. The lack of full weld penetration would act to concentrate and magnify whatever stresses were acting in this area of the manway.

There was another aspect of stresses in the tank related to the liquid being stored. Up until about a year before the failure, gasoline, having a specific gravity of approximately 0.73, was stored in the tank. Then crude oil, with a specific gravity of about 0.91, replaced the gasoline. This 18% increase in stored liquid density represented an approximate increase in static head pressure and applied stress of about 25%.

In conclusion, this tank ruptured by brittle fracture at the manway neck weld due to the interaction of multiple causitive effects. The brittle condition of the steel was a result of the use of the tank in ambient temperatures that were far below the measured ductile-to-brittle transistion temperature of the material. The DBTT values might have been lower, and made brittle fracture somewhat less likely, if the manganese and carbon percentages in the steel composition had resulted in a Mn-to-C ratio that was at least 3.0, but this was not the reality. In addition, applied stresses in the manway area of the tank were intensified due to three findings. First, the uneven thermal expansion and contraction between the base floor plates and vertical wall steel due to exposure to different temperatures created additive bending stress. Second, the lack of full penetration of the weld between the manway neck and pad created a stress concentration that would accelerate crack initiation. Finally, the relatively recent storage of the higher density oil in the tank created an overall increase in applied stresses of about 25% .

Recommendations for corrective actions to avoid a similar future failure at this location were not explicitly covered in the article cited by Dr. LeMay. However, the present author believes the following minimum actions would have been appropriate:

- Specify and use steel having a DBTT that is lower than the lowest anticipated ambient temperature at the site.
- Design the tank for the highest density liquid that might be stored in it. Assure that all welding personnel and procedures were certified and that all finished welds were inspected and approved before acceptance of a replacement tank.

The following is a brief list of statements describing other types of failures or problem situations a person performing RCFA's might confront in metallurgical or mechanical areas:

- Possible microbiological influened corroison(MIC) in a cooling water piping system.
- Abnormal centrifugal pump operation that may be due to a mis-match between the downstream hydraulic piping system and the pump's capabilities, cavitation, impeller corrosion, etc.
- Possible hydrogen embrittlement and cracking failure of an electrochemically plated steel component due to a deficient post-plating bake out process that might have been used.
- Stress-corrosion cracking of a Type 304 stainless steel pressure vessel's head potentially caused by the thermal insulation applied that contained a high concentration of chlorides.
- Fretting wear that lead to fatigue failure of certain tubes in a shell & tube heat exchanger due to flow-induced vibrations between particular tubes and the baffle plates used.
- Premature fatigue failure of a rotating shaft due to a series of brief operating stress excursions well above the endurance limit of the shaft material even though most operation was below that limit.
- Galvanic corrosion of an aluminum aircraft component due to possible wetted contact with protruding graphite fibers from a nearby fiber-reinforced composite material component.
- Failure of the bearings on the shaft of a large centrifugal compressor potentially due to water in the system supplying lubrication to the bearings.

- Crevice or pitting corrosion of a marginally resistant stainless steel, for the given electrolyte, in a near "dead leg", low velocity section of a piping system.

- Failure of a cast iron valve in a piping system potentially due to defects in the casting coupled with a quick-closing upstream valve and the resulting water hammer effect.

- Leaks on the tubesheet face of a sheet and tube heat exchanger potentially due to incorrect tube material selection and shell-side corrosion, inadequate rolling of the tubes into the tubesheet or lack of quality seal welds around the tubes on the tubesheet's outer surface.

- Abnormal numbers of domestic air-conditioning unit failures and electronic appliance failures in private homes with a particular type of installed drywall (sheetrock) material from China.